



EFFECTIVE FEATURE EXTRACTION METHOD FOR UNCONSTRAINED ENVIRONMENT: LOCAL BINARY PATTERN OR LOCAL TERNARY PATTERN

MUTHUSAMY RAJEEV KUMAR¹, RAMKUMAR SUNDARAM², MAGESWARAN RENGASAMY³,
RAVICHANDRAN BALAKRISHNAN⁴

Keywords: Local binary pattern; Local ternary pattern; Feature extraction; Machine learning; Unconstrained environment; Noncooperation.

In this study, a range of algorithms addressing the challenges posed by noise and illumination were investigated. Two algorithms, namely LTP and LBP, were selected for comparison due to their demonstrated effectiveness. The process becomes time-consuming due to training samples, mainly when dealing with images featuring higher levels of noise and illumination variations, necessitating efficient algorithms for effective recognition. To compare two effective feature extraction methods viz local binary pattern (LBP) and local ternary pattern (LTP) for an unconstrained environment. The impact of noise and illumination factors is particularly pronounced in the iris datasets of non-cooperative subjects, which serve as the input images for this analysis. These algorithms were applied to diverse datasets with distinctive illumination properties to facilitate feature extraction. The results indicated that the LTP exhibited efficiency in comparison, suggesting its efficacy in handling datasets with varying illumination characteristics. A comparative analysis between LBP and LTP was conducted on two distinct datasets, namely UBIRIS and CASIA. The investigation into the sensitivity of LTP revealed heightened sensitivity during the performance analysis test, with consistent accuracy observed at 50 samples and a scale of 0.3. In the case of the CASIA iris dataset, the recall of LTP and LBP exhibited nearly identical accuracy levels, converging after 70 samples for non-cooperative iris datasets compared to the LBP.

1. INTRODUCTION

Iris image processing uses methods to examine and glean data from photographs of the human iris as a topic of study and application. The iris, or colorful part of the eye surrounding the pupil, varies from person to person. There are several significant uses for iris image processing, including biometric identification, secure access control, healthcare and its monitoring, time and attendance tracking, human-computer interaction, forensic science, personal device security, financial transactions, border control, and immigration. Iris recognition [7] is among the most trustworthy biometric identification methods. The iris' distinctive features, including its crypts, furrows, and collarette, can be photographed and used for identification and authenticity. It confirms a person's identification in security systems, access controls, and border controls. In high-security settings where access control is essential, like governmental buildings, data centers, and research labs, iris recognition is frequently utilized. Presenting their irises for authentication allows users to enter locations that are prohibited. Organizations can measure time and attendance by using iris image processing. Using iris recognition, employees can clock in and out, removing the chance of time theft and improving the accuracy of attendance records. Some nations utilize iris recognition as part of their immigration and border control procedures to confirm travelers' identities and find potential security risks. In the context of mobile banking and payment systems, iris recognition can improve the security of financial transactions.

It adds a layer of biometric authentication to safeguard against unwanted account access. For safe unlocking, iris recognition can be embedded into laptops, tablets, and smartphones. This technology can guard against illegal access to devices and safeguard personal data. Forensic investigations

can utilize iris image processing to identify people using iris photographs discovered at crime sites. When other means of identification are unavailable, it can also be used to confirm the identity of those who have passed away. Systems for human-computer interaction that are more secure and practical can be made using iris recognition technology. Iris scanning can confirm a person's identification and facilitate private data access. For example, a computer that can authenticate a person by scanning their iris can make it easier to access private data. Changes in the iris' structure and features might indicate several medical diseases, including diabetes or specific genetic abnormalities. The early detection and monitoring of such conditions can be aided by iris image processing. Iris image processing is used in these applications to take high-resolution iris photos, extract pertinent features, and compare those features to a database of previously registered iris patterns. The use of iris recognition as a biometric authentication method has increased dramatically because of image processing and computer vision technology development.

Iris image segmentation, which divides the iris region from the remainder of the eye image, is essential in iris identification and image processing applications. The following factors and difficulties, however, can make it a difficult task:

- Iris size and position variability: The iris's size and location in the eye can change significantly between people and even within an individual's image. Due to this variability, creating a segmentation technique that can be used for all data is challenging.
- Pupil dilation: Changes in illumination conditions and physiological factors can cause pupil size variations. If the pupil is small or irregularly shaped, it can be difficult to tell the difference between the iris and the pupil.

¹ Department of CSE, Vel Tech Rangarajan Dr. Sagunthala R&D Institute of Science and Technology, Avadi, Chennai – 600062, Tamil Nadu, India. E-mail: smrajeevkumar@gmail.com, drmrajeekumar@veltech.edu.in

² Department of Electronics and Communication Engineering, Sri Eshwar College of Engineering Coimbatore – 641202, Tamil Nadu, India. E-mail: sram0829@gmail.com, ramkumar.s@sece.ac.in

³ Department of Electrical and Electronics Engineering, S. A. Engineering College, Chennai – 600077, Tamil Nadu, India. Email: mageswaranrr@gmail.com, mageswaran@saec.ac.in

⁴ Department of Robotics and Automation Engineering, Vel Tech Multi Tech Dr. Rangarajan Dr. Sakunthala Engineering College, Chennai – 600062, Tamil Nadu, India. Email: balakrishnan007r@gmail.com, balakrishnan@veltechmultitech.org

- **Eyelashes and eyelids:** Because eyelashes and eyelids frequently overlap the iris and may have similar colors and textures, it can be challenging to segregate them from the iris region.
- **Iris texture:** The intricate and complex iris can have crypts, furrows, and collarettes, among other patterns. During segmentation, these patterns can occasionally be misinterpreted with noise.
- **Blur and defocus:** Iris photos may be blurry or out of focus due to motion blur or the camera's focus capabilities. Such fuzziness can cause inaccurate segmentation.
- **Occlusion:** Segmentation can be hampered by impediments in front of the iris, such as eyeglasses or contact lenses. These items might cause noise in the segmentation process and partially block the iris's field of view.
- **Image quality variability:** The iris's image quality might differ based on image resolution, lighting, and camera settings. Low-quality images may not have enough information for accurate segmentation.
- **Sclera and limbus:** In some photographs, the iris and sclera (the white component of the eye) may not always be distinguished. Because of this ambiguity, segmentation may be complex.
- **Non-uniform illumination:** Uneven lighting conditions can cause iris brightness and contrast variations, making it more challenging to separate the iris from its surroundings.

To address these challenges in iris picture segmentation, robust and adaptable segmentation algorithms that can cope with changes in iris appearance and environmental factors are frequently necessary. The accuracy of iris segmentation has been improved by using advanced computer vision algorithms, such as machine learning and deep learning [28], to an extensive collection of iris images and the ground truth segmentations accompanying them. Before segmentation is carried out, additional preprocessing operations like picture improvement and quality assessment can lessen some of these difficulties.

2. LITERATURE REVIEW

A multiscale median LTP (MLTP) framework [12] was proposed by Ji et al. to improve the local ternary pattern's performance in noisy texture categorization [14,19]. The method was initially constructed using a non-overlapping median sampling methodology to reduce noise. The descriptors, such as central, radial, and magnitude, are then re-defined for MLTP. Additionally, a uniform three-pattern mapping solution that is rotation-invariant has been put forth to facilitate the extrapolation of original MLTP codes from high-dimensional to low-dimensional patterns. Additionally, they showed that MLTP, in conjunction with support vector machines, enhanced accuracy and noise resilience compared to alternative approaches. Zhilai et al. employed the local binary pattern (LBP) for facial recognition [3] when lights were used to take nighttime photos of the subjects. Using the local enhancement process in conjunction with LBP, performance degradation owing to lighting impact has been addressed. According to their experimental results, the accuracy of facial recognition with lighting effect has improved from 42.18% to 58.62%.

A comprehensive study on the applications of facial image

analysis in LBP [25] has been conducted by Ma et al. They described the various LBP variations and their attributes based on (i) increasing discriminative ability (ii) increasing robustness (iii) selecting the neighborhood (iv) extending to 3D, and (v) combining with other features [26]. They also compiled the core face feature matching algorithms and their stated accuracy on the FERET dataset. The LBP approach was better suited for facial identification [4,11,23], particularly in extreme lighting changes and blurred and noisy images. Beli and Guo [6] classified the face features derived by LBP using the k-nearest neighbor technique. This algorithm combination has been implemented for significant variations [24] in input images such as aging, expression, illumination, inaccurate alignment, and possible. The proposed algorithm was tested on the CMU PIE and LFW datasets and performed well. Scale-invariant LTP (SILTP) was proposed by Mahaboob and Reddy [20] to make the LBP resistant to changes in illumination and noise. A generalized local ternary pattern (gLTP) was designed to capture edge and blob-like features. They discovered that the gLTP method outperformed all other methods and was resistant to noise and changes in illumination. LTP has been utilized by Rampun et al. [2] to identify cancer using breast density classification. Table 1 refers to the overview of the associated research work.

Table 1
Overview of associated research works

Method	Objective	Training set/ Application
Multiscale median LTP(MLTP) with SVM	Improved accuracy and noise robustness over other methods. Performance	Facial Recognition
LBP	Degradation owing to lighting impact	Facial Recognition
LBP	Extreme lighting changes, blurred and noisy images	Facial Recognition Technology (FERET) dataset
LBP with k-nearest neighbor algorithm	Large variations in input images such as aging, expression, illumination, inaccurate alignment	Facial Dataset and Labeled Faces in the Wild Home (LFW) datasets
Generalized local ternary pattern (gLTP)	Resilient to both noise and illumination change	Facial Recognition

3. METHODS

Most image processing techniques start with acquiring the input image and are followed by pre-processing stages such as crop, resizing, and noise removal. In the next stage, the process narrows down with the segmentation level. The level set approach and particle swarm optimization (PSO) [27] are combined in the picture segmentation method known as RBLs (region-based level set with PSO) with PSO. This method automatically divides an image into interesting areas or objects.

3.1. ESSENTIAL ELEMENTS OF RBLs WITH PSO

The level set method (LSM) is a mathematical framework for segmenting images and modeling shapes. It uses a level set function to represent the evolving boundaries of things. This function divides the image into areas over time. The level set function is used in the context of RBLs with PSO to represent the changing boundaries of the places or objects to be segmented. Region-Based Segmentation: The term

"region-based segmentation" (RBLs) denotes a segmentation method that divides an image into regions [15] or objects according to their attributes, such as intensity or texture. This contrasts with edge-based segmentation, which depends on spotting sudden changes in gradients or intensity. PSO is a population-based optimization system motivated by the cooperative behavior of fish or birds. PSO is utilized as an optimization technique in the context of RBLs to direct the evolution of the level set function. PSO searches for the ideal arrangement of a set of particles in the solution space. These particles are used in RBLs with PSO to affect the level set function's evolution and aid in its convergence to an optimal segmentation. In image processing, pupil segmentation removes the pupil—the dark circular opening at the center of the eye's iris—from an eye image or a video frame. In many applications, including gaze tracking, biometric verification, and medical diagnostics, precise pupil segmentation is crucial.

3.2 LOCAL BINARY PATTERN

Using a straightforward yet powerful texture operator called LBP, each pixel in an image is labeled by thresholding its surrounding region and interpreting the result as a binary integer. The LBP texture operator [5] has gained popularity in many applications due to its ease of calculation and ability to discriminate. Texture analysis' traditional disparate structural and numerical frameworks can be understood as a unifying process. The LBP operator's robustness in monotonous grayscale shifts, such as those caused by lighting variances, is possibly the most crucial feature for applications. Its computational simplicity is another noteworthy feature [17] that enables image interpretation in challenging real-time scenarios. The visual descriptor type can be used for categorization in computer vision. Furthermore, there is a significant improvement in the detection performance when the visual descriptor [8] and the histogram of gradients (HoG) are combined. Figure 1 shows the three neighborhood samples used to determine an LBP and create a texture [18].

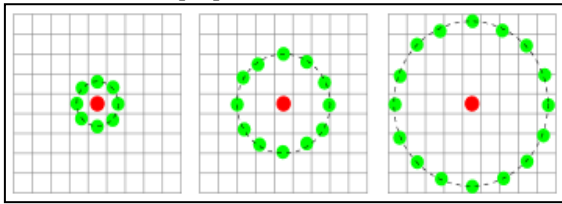


Fig. 1. Texture definition and LBP calculation using three neighborhood examples.

1. Create cells using the window under consideration (e.g., 16x16 pixels for each cell).
2. Compare each of a cell's eight neighbors—left, middle, left-below, right-top, *etc.*—with each pixel in the cell. Rotate the pixels either clockwise or counterclockwise.
3. If the value of the center pixel is higher than the value of the neighboring pixel, assign "0". If not, type "1." It offers an eight-digit binary number typically converted to decimal for ease of use.
4. Determine the probability of occurrence of any "number" that can be seen as a 256-dimensional vector characteristic as a histogram over the cell, that is, every combination of pixels that is less or greater than the center.

If necessary, normalize the histogram.

5. To get a feature vector for the whole window, combine all cell histograms.

Machine learning methods like support vector machines, which can be utilized for texture analysis, should be employed to classify the processed images. To shorten the feature vector, it is further divided into two categories: uniform patterns and non-uniform patterns. This can be estimated depending on the number of transitions, such as 0 to 1 or 1 to 0. If the count is no more than two, it is referred to as a uniform pattern; otherwise, it is referred to as a non-uniform pattern. Figure 2 depicts an example of the LBP calculation. It's also clear from the generated result that the binary pattern will be categorized as a uniform pattern.

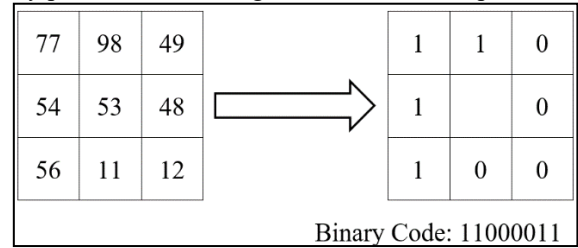


Fig. 2 – LBP calculation.

3.3 LOCAL TERNARY PATTERN

The Local Ternary Pattern (LTP) [21] is the noise-resistant version of the LBP [10, 13]. Both methods encode the intensity difference between the center pixel and its neighbors. LBP is noise-sensitive, particularly in smooth areas, since a little grey level shift of the central pixel could produce different codes for a neighborhood in an image. LTP addresses the noise sensitivity problem that besets LBP by storing the minute change in pixels into a third state. LTP thresholds pixels into three values rather than just one using a threshold constant, as in LBP. A 3x3-pixel block segmented output image is subjected to LTP operator operations. In this block, the trinary code represents the difference between the center and the adjacent pixel. The letters g, c and k to stand for the threshold constant, neighboring pixels, and the center pixel's gray level, respectively. The LTP function is

$$LTP = \sum_{n=0}^7 f(g, c, k) 3^n, \quad (1)$$

where $f(g, c, k)$ is the threshold function, which has the definition provided by

$$f(g, c, k) = \begin{cases} 1, & \text{if } g \geq c + k, \\ 0, & \text{if } g > c - k \text{ and } g < c + k, \\ -1, & \text{if } g < c - k. \end{cases} \quad (2)$$

Additionally, the *LTP* will be divided into positive, as shown in Equation (3), and negative LBP, as shown in eq. (4) using the following coding method to reduce the feature dimension:

$$f_{po}(g, c, k) = \begin{cases} 1, & \text{if } g \geq c + k \\ 0, & \text{Otherwise} \end{cases} \quad (3)$$

$$f_{na}(g, c, k) = \begin{cases} 1, & \text{if } g \leq c - k \\ 0, & \text{Otherwise} \end{cases} \quad (4)$$

Positive and negative discriminative features will be generated from the segmented output image. In this piece, a 2x2 pixel represents each unique block. The LTP code for each block is stored in a separate histogram.

78	99	50	(Threshold $k=5$)	1	1	0
55	54	49		0		0
57	12	13		0	-1	-1

Ternary Code: 1100(-1)(-1)00

Fig. 3 – LTP calculation.

Figures 3 and 4 illustrate the LTP computation in action.

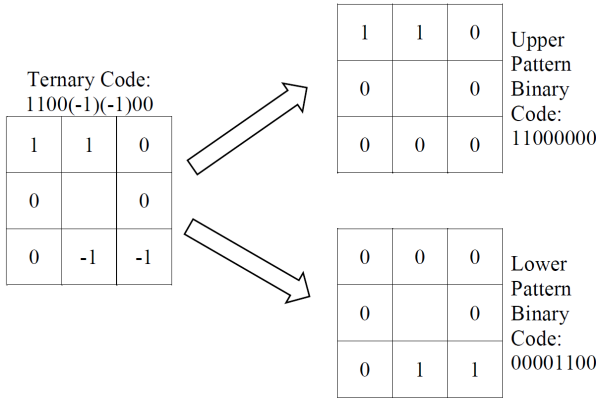


Fig. 4 – Example of separating the LTP code into positive and negative code.

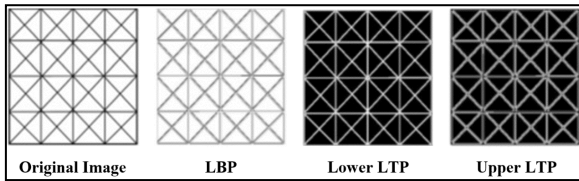


Fig. 5 – Illustration of LBP and LTP on the reference image.

Figure 5 shows the application of LBP and LTP to the original image. By concatenating and combining the different LTP code histograms, a single composite feature histogram is created. Principal component analysis (PCA), which converts the high-dimensional histogram feature vector to a lower-dimensional one, is then used to reduce the complexity.

4. RESULTS AND DISCUSSION

The suggested methodology was applied to several iris datasets to estimate its performance, including UBIRIS [22], CASIA V4-Interval, CASIA V4-Lamp, and CASIA V4-twin [16]. Regarding the datasets above, the output of our methodology's segmentation step is shown in that order in Figs. 6, 7, 8, and 9. The prime objective of this performance estimation is to ensure the effectiveness of the proposed methodology among the various iris datasets. As the effectiveness of the segmentation resulted in the perfect identification of the iris portion, verifying the proposed feature extraction methods was beneficial, viz. LBP and LTP. As segmentation plays a vital role in iris recognition, an effective method for this is provided in Fig. 6. The main issue with LBP is its sensitivity to noise. However, since much of recent research focuses on non-cooperative environments, the limitations of LBP can be significantly addressed by using LTP.

The suggested approach has been applied to several iris datasets, as shown in Fig. 7 through 10. where the matching

output images of the segmentation are (b) and (d), and the input images are (a) and (c).

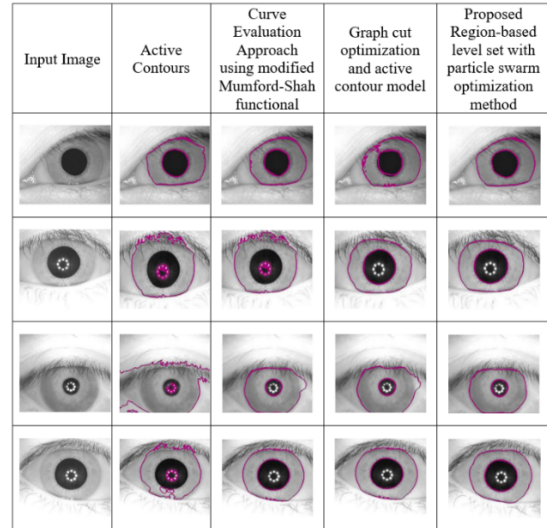


Fig. 6 – Efficient division technique for non-cooperative iris identification and a comparison with current approaches.

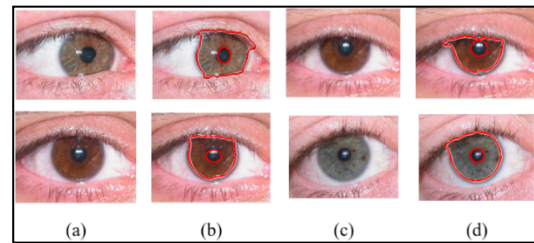


Fig. 6 - (a), (c) UBIRIS dataset, (b), (d) Segmentation output with respect to (a) and (c).

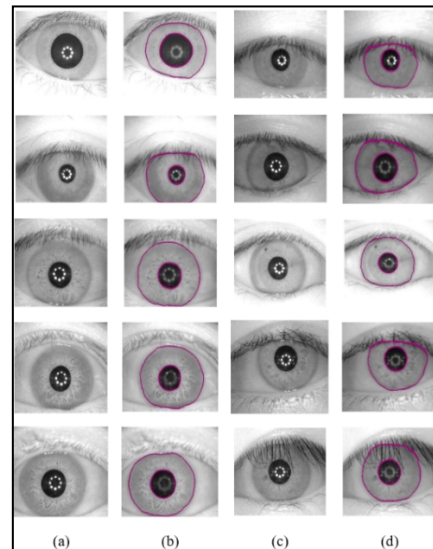


Fig. 8 - (a), (c) CASIA V4-Interval dataset, (b), (d) Segmentation output with respect to (a) and (c).

Despite a problem with the dataset's lighting, the suggested approach performed better when applied to the CASIA V4-Interval dataset, and the experimental outcomes are shown in Fig. 8. The images taken under the unconstrained environment [1,9] were found from the CASIA V4-Lamp dataset. The segmentation results shown in Fig. 8 evidence the proposed segmentation algorithm's performance.

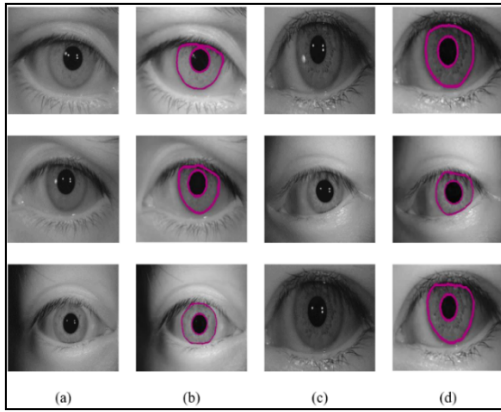


Fig. 9 – (a), (c) CASIA V4-Lamp dataset, (b), (d) Segmentation output with respect to (a) and (c).

The output of the normalizing step is passed into the feature extraction step. This improved normalized image is subjected to the LTP operator, which yields two positive and two negative LBP images. These are then used to extract discriminative features from the segmented iris image. To preserve the iris's local feature and spatial position data, the suggested work splits the iris into the necessary number of blocks to produce a high-dimensional LTP feature.

Furthermore, every block has a 2×2 pixel size, and a histogram records whether the LTP code for each block is present. The LTP upper and lower 2×2 blocks, and their respective histograms are shown in Fig. 11 and 12. The upper and lower LTP histograms are combined to create the final histogram, displayed in Fig. 13. Exploiting the advantages of LBP and LTP applications led the researchers to implement various related applications. In our case, we have implemented the feature extraction stage of non-cooperative iris recognition. The reason behind this implementation was the input images were captured without the support of the individuals. The noise factors with more illumination may directly affect the recognition accuracy.

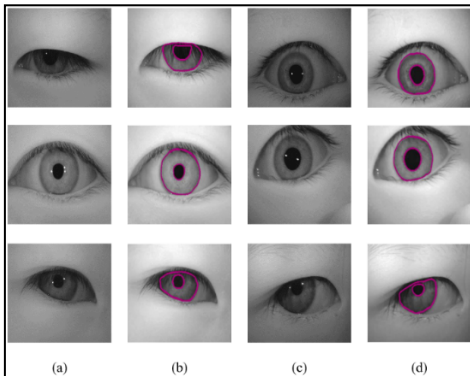


Fig. 10 – (a), (c) CASIA Twin dataset, (b), (d) Segmentation output with respect to (a) and (c).

Figures 13 and 14 show the performance comparison of the LBP and LTP using two distinct iris data sets, namely UBIRIS and CASIA. As the UBIRIS dataset is more specific to the non-cooperative situation, there may be less accuracy in Fig. 13 compared with Fig. 14. The following figures clearly show that as the number of training samples increases, the recognition system's accuracy improves. In both datasets, the LTP has outperformed the LBP. Even though in most of the cases, the LTP outperforms the LBP, the accuracy of the LBP is also dominating in the rare cases, which are also seen in Fig. 13 and Fig. 14. This may be due

to the quality of the input image and needs more concentration by the researchers of this field.

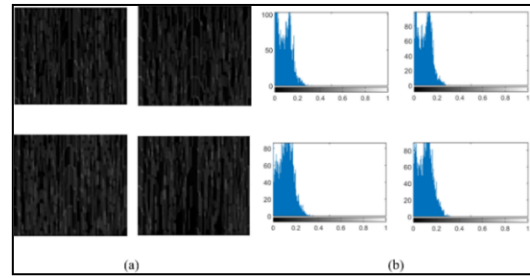


Fig. 11 – (a) 2×2 blocks of LTP upper image, (b) 2×2 histogram blocks of LTP upper image.

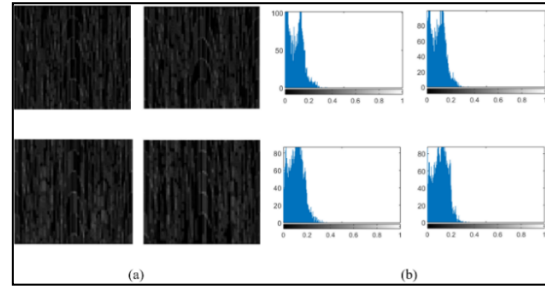


Fig. 12 – (a) 2×2 LTP lower image blocks and 2×2 LTP lower image histogram blocks.

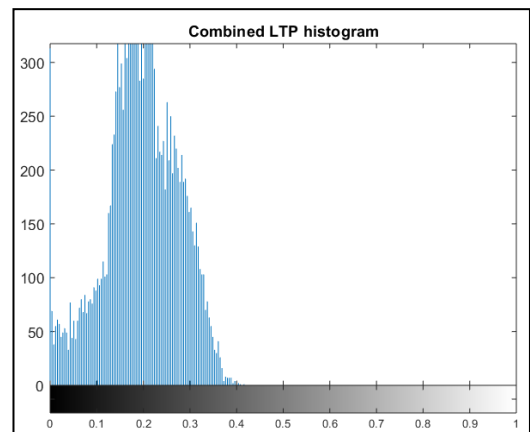


Fig. 13 – Combined LTP histogram.

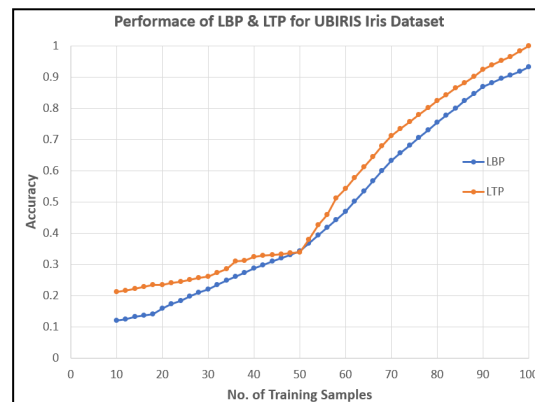


Fig. 14 – Performance of LBP and LTP for UBIRIS iris dataset.

The proposed research has been carried out for iris recognition using various datasets such as CASIA, UBIRIS, UPOL, etc. This work also emphasizes the difference in illumination due to the capturing environment, such as cooperation and non-cooperation.

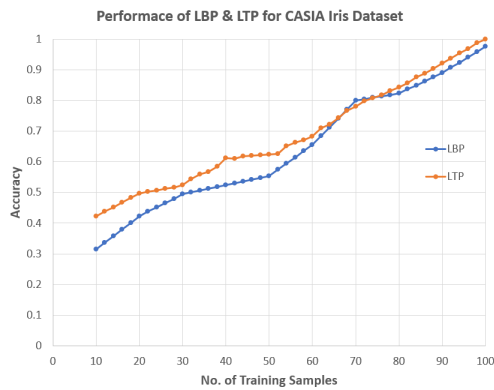


Fig. 15 – Performance of LBP and LTP for CASIA iris dataset.

Similarly, the LTP benefits from splitting the upper region, lower region, and combined histogram. Table 2 provides the recognition rates concerning these regions.

Table 2

The classification rate of various regions concerning LBP and LTP.

Operator	Classification rate (%) for various regions		
	Lower Region	Upper Region	Combined Region
LBP	74.63	82.43	88.23
LTP	91.23	88.46	96.42

The classification rate of the lower region shall vary based on the illumination parameter of the input image, especially in non-cooperative situations. However, as Table 2 illustrates, the categorization rate for the combined region will be higher.

5. CONCLUSIONS

Modern society heavily relies on biometrics, particularly security, identification, and access control. Several topologies exist in biometrics, but iris imaging is the most significant entity. The unique quality of iris images is that when divided into several divisions, none will match the others. Images with higher levels of noise and illumination could need a more efficient algorithm to identify them. In this work, several noise factor and illumination-related algorithms were investigated, and two efficient methods, LBP and LTP, compared to LBP and LTP, are better suited for the feature extraction and classification stages of image processing techniques; hence, these stages have received the most attention. The accuracy and performance of LBP and LTP for the CASIA iris dataset were almost similar after 70 samples. A comparison between LBP and LTP was performed for two different datasets, UBIRIS and CASIA. The LTP is highly sensitive and was investigated during the performance analysis test, and the accuracy was the same at 50 samples with an accuracy of 0.3 scales.

Received on 22 April 2024

CREDIT AUTHORSHIP CONTRIBUTION STATEMENT

M. Rajeev Kumar: Formal analysis, Literature Review, Data acquisition, Data organization, Implementation, writing—original manuscript and preparation.

S. Ramkumar: measurement methodology, experimental platform design, Data consistency analysis, and verification.

R. Mageswaran: Data collection, Reviewing and editing the manuscript, Literature review.

R. Balakrishnan: conceptualization, software development, writing—manuscript review and editing, Validation, Investigation.

REFERENCES

1. A.F.M. Raffei, H. Asmuni, R. Hassan, R.M. Othman, *Feature extraction for different distances of visible reflection iris using multiscale*

- sparse representation of local Radon transform*, Pattern Recognition, **46**, 10, pp. 2622–2633 (2013).
2. A. Rampun, P. Morrow, B. Scotney, J. Winder, *Breast density classification using local ternary patterns in mammograms*, In Int. Conf. Image Analysis and Recognition, **1**, pp. 463–470 (2017).
3. A.F. Zhilali, M. Nasrun, C. Setianingsih, *Face recognition using local binary pattern (LBP) and local enhancement (LE) methods at night period*. Inter. Conf. on Industrial Enterprise and System Engineering (Atlantis Press) (2018), **1**, pp. 103–108 (2019).
4. B. Zhang, Y. Gao, S. Zhao, J. Liu, *Local derivative pattern versus local binary pattern: face recognition with high-order local pattern descriptor*, IEEE Trans. on image processing, **19**, 2, pp. 533–544 (2009).
5. D. Huang, C. Shan, M. Ardabilian, Y. Wang, L. Chen, *Local binary patterns and its application to facial image analysis: a survey*, IEEE Trans. on Systems, Man, and Cybernetics, Part C (Applications and Reviews), **41**, 6, pp. 765–781 (2011).
6. I.L. KambiBeli, C. Guo, *Enhancing face identification using local binary patterns and k-nearest neighbors*, J. of Imaging, **3**, 3, pp. 37–49 (2017).
7. J.R. Malgheet, N.B. Manshor, L.S. Affendey, *Iris recognition development techniques a comprehensive review*, Complexity, pp. 1–32 (2021).
8. J. Ren, X. Jiang, J. Yuan, *A chi-squared-transformed subspace of LBP histogram for visual recognition*, IEEE Trans. on Image Processing, **24**, 6, pp. 1893–1904 (2015).
9. K. Nguyen, C. Fookes, S. Sridharan, *Constrained design of deep iris networks*, IEEE Trans. on Image Processing, **29**, pp. 7166–7175 (2020).
10. K. Wang, A. Kumar, *Cross-spectral iris recognition using CNN and supervised discrete hashing*, Pattern Recognition, **86**, pp. 85–98 (2019).
11. K.S. Reddy, V.V. Kumar, B.E. Reddy, *Face recognition based on texture features using local ternary patterns*, Int. J. of Image, Graphics and Signal Processing, **7**, 10, pp. 37–45 (2015).
12. L. Ji, Y. Ren, X. Pu, G. Liu, *Median local ternary patterns optimized with rotation-invariant uniform-three mapping for noisy texture classification*, Pattern Recognition, **79**, pp. 387–401 (2018).
13. L. Liu, P. Fieguth, Y. Guo, X. Wang, M. Pietikäinen, *Local binary features for texture classification: Taxonomy and experimental study*, Pattern Recognition, **62**, pp. 135–160 (2017).
14. L. Liu, S. Lao, P.W. Fieguth, Y. Guo, X. Wang, M. Pietikäinen, *Median robust extended local binary pattern for texture classification*, IEEE Trans. on Image Processing, **25**, 3, pp. 1368–1381 (2016).
15. M. Huang, Z. Mu, H. Zeng, S. Huang, *Local image region description using orthogonal symmetric local ternary pattern*, Pattern Recognition Letters, **54**, pp. 56–62 (2015).
16. ***National Laboratory of Pattern Recognition (NLPR) | Institute of Automation, Chinese Academy of Sciences (CASIA),
17. S. Murala, R.P. Maheshwari, R. Balasubramanian, *Local tetra patterns: a new feature descriptor for content-based image retrieval*, IEEE Trans. on image processing, **21**, 5, pp. 2874–2886 (2012).
18. S. Wang, Q. Wu, X. He, J. Yang, Y. Wang, *Local N-Ary pattern and its extension for texture classification*. IEEE Trans. on Circuits and Systems for Video Technology, **25**, 9, pp. 1495–1506 (2015).
19. S. Wu, L. Yang, W. Xu, J. Zheng, Z. Li, Z. Fang, *A mutual local-ternary-pattern based method for aligning differently exposed images*, Computer Vision and Image Understanding, **152**, pp. 67–78 (2016).
20. S.T. Mahaboob, S.N. Reddy, *Comparative performance analysis of LBP and LTP based facial expression recognition*. Int. J. of Applied Engineering and Research, **12**, 17, pp. 6897–6900 (2017).
21. T.H. Rassem, B.E. Khoo, *Completed local ternary pattern for rotation invariant texture classification*, Scientific World Journal (2014).
22. ***University of Bath Iris Image Database.
23. W. Yang, Z. Wang, B. Zhang, *Face recognition using adaptive local ternary patterns method*, Neurocomputing, **213**, pp. 183–190 (2016).
24. X. Wu, J. Sun, G. Fan, Z. Wang, *Improved local ternary patterns for automatic target recognition in infrared imagery*, Sensors, **15**, 3, pp. 6399–6418 (2015).
25. Y. Ma, Z. Huang, X. Wang, K. Huang, *An overview of multimodal biometrics using the face and ear*, Mathematical Problems in Engineering, pp. 1–17 (2020).
26. Z. Guo, X. Wang, J. Zhou, J. You, *Robust texture image representation by scale selective local binary patterns*, IEEE Trans. on image processing, **25**, 2, pp. 687–699 (2015).
27. M.I. Abdelwanis, R. El-Sehiemy, M.A. Hamida, *Parameter estimation of permanent magnet synchronous machines using particle swarm optimization algorithm*, Rev. Roum. Sci. Techn. Serie Electrotechn. et Energ., **64**, 4, pp. 377–382 (2022).
28. B.R.C. Joseph, I.J. Jebadurai, G.J.L. Paulraj, J. Jebadurai, M.M. Varuvel, *Deep Vein Net: Deep vein thrombosis identification via sooty tern optimized deep learning network*, Rev. Roum. Sci. Techn. Serie Electrotechn. et Energ., **69**, 1, pp.115–120 (2024).